



Computational study of energy transfer in two-dimensional J-aggregates

Lazaros K. Gallos^a, Panos Argyrakis^{a,*}, A. Lobanov^b, A. Vitukhnovsky^b

^a*Department of Physics, University of Thessaloniki, 54124 Thessaloniki, Greece*

^b*Laboratory of Luminescence, P.N. Lebedev Physical Institute, Russian Academy of Sciences, 119991 Moscow, Russia*

Available online 22 September 2004

Abstract

We perform a computational analysis of the intra- and interband energy transfer in two-dimensional J-aggregates. Each aggregate is represented as a two-dimensional array (LB-film or self-assembled film) of two kinds of cyanine dyes. We consider the J-aggregate whose J-band is located at a shorter wavelength to be a donor and an aggregate or a small impurity with longer wavelength to be an acceptor. Light absorption in the blue wing of the donor aggregate gives rise to the population of its excitonic states. The depopulation of these states is possible by (a) radiative transfer to the ground state, (b) intraband energy transfer, and (c) interband energy transfer to the acceptor. We study the dependence of energy transfer on properties such as the energy gap, the diagonal disorder, and the exciton–phonon interaction strength. Experimentally observable parameters, such as the position and form of luminescence spectrum, and results of the kinetic spectroscopy measurements strongly depend upon the density of states in excitonic bands, rates of energy exchange between states and oscillator strengths for luminescent transitions originating from these states.

© 2004 Elsevier B.V. All rights reserved.

PACS: 71.35.Aa; 78.66.Qn; 78.30.Ly

Keywords: Frenkel excitons; J-aggregates; Exciton transport

1. Introduction

During recent years, J-aggregates of cyanine dyes have attracted a lot of interest, since they

exhibit important and unusual optical properties [1,2]. These properties are mainly due to the delocalization of the Frenkel excitons over a number of molecules, resulting in narrow absorption and emission peaks. The chromophores in a J-aggregate can be arranged in a linear one-dimensional chain or on a two-dimensional planar structure.

*Corresponding author. Tel.: +30-231-0998043; fax: +30-231-0998042.

E-mail address: panos@physics.auth.gr (P. Argyrakis).

Although excited state dynamics of the J-aggregates have been widely studied, the key structural and energetic transport properties remain unclear so far. Detailed studies of one-dimensional disordered chains can be found, e.g., in Refs. [3–5]. In this work we study the mechanisms of energy transfer in two-dimensional J-aggregates, where an acceptor molecule is placed in the middle of a matrix of donors.

2. The model

The Hamiltonian of the aggregated system is constructed according to a method similar to that of Schreiber and Toyozawa [6], with two main modifications: (a) we are taking into account all the intermolecular interactions among all possible pairings of the N molecules comprising the aggregate and (b) we are treating the dipole moment of the molecular transition as a vector. The Hamiltonian of the system is represented as

$$H = \sum_{n=1}^N (E_n^{\text{mono}} + D_n) |n\rangle \langle n| + \sum_{n=1}^N \sum_{m=1, m \neq n}^N V_{n,m} |m\rangle \langle n|. \quad (1)$$

In this expression, E_n^{mono} is the energy of the n th monomer molecular transition, D_n represents the static disorder caused by the influence of the molecule neighborhood, and $|n\rangle$ is the state where all molecules are in the ground state with the exception of the n th molecule, which is in the excited state. The intersite interactions $V_{n,m}$ are calculated according to the extended dipole approximation [7].

The energy levels of the system E_i ($i=1, N$) are found from the eigenvalues of this Hamiltonian, with the corresponding eigenfunctions

$$|\psi_i\rangle = \sum_{n=1}^N a_{i,n} |n\rangle, \quad (2)$$

obtained from the eigenvectors $\vec{a}_i = (a_{i,1}, \dots, a_{i,N})$ of the same Hamiltonian.

The aggregate transition dipole moments are given by

$$\vec{\mu}_i = \sum_{n=1}^N a_{i,n} \vec{\mu}_n^{\text{mono}}, \quad (3)$$

where $\vec{\mu}_n^{\text{mono}}$ is the single molecule transition dipole moment of the n th monomer. The oscillator strength f_i associated with a given eigenstate i is proportional to the squared magnitude of the transition moment dipole

$$f_i \sim |\mu_i|^2 f_0. \quad (4)$$

The line-shape of the absorption spectrum A as a function of the energy E is given by [8]

$$A(E) \equiv \frac{1}{N} \left\langle \sum_{i=1}^N \mu_i^2 L(E - E_i) \right\rangle, \quad (5)$$

where $L(E - E_i)$ represents a Lorentzian curve centered in E_i , with a width of 20 cm^{-1} at half-height that represents the natural line-width of the peak. The height of the peak is proportional to the oscillator strength of the associated eigenstate, as can be seen in Eq. (5). The average in Eq. (5) takes place over all realizations of the disorder, as will be described below. The resulting absorption is calculated for the natural polarization of the incident light.

The eigenstates E_k are mixed through exciton–phonon interactions, so that the transitions from the exciton state k to the state k' become allowed, along with the creation of a phonon ρ on the molecule n with frequency $\hbar\omega_\rho = E_k - E_{k'}$. In the first-order perturbation theory [9,10], using the wavefunction form of Eq. (2), the matrix element of the transition is

$$\langle k' | \hat{H}_{\text{int}} | k \rangle = g_\rho a_{k',n}^* a_{k,n} \sqrt{\bar{n}_\rho + 1}, \quad (6)$$

where g_ρ is the exciton-phonon coupling constant and \bar{n}_ρ is the phonon occupation number. For the phonon absorption ($E_k < E_{k'}$), in Eq. (6) one has $\sqrt{\bar{n}_\rho}$ instead of $\sqrt{\bar{n}_\rho + 1}$. We take \bar{n}_ρ to correspond to a Bose distribution with temperature T

$$\bar{n}_\rho(T) = \frac{1}{\exp(\hbar\omega_\rho/T) - 1}. \quad (7)$$

We assume the phonon states ρ to form a continuum. Then the hopping rate for the

phonon-assisted transition $k \rightarrow k'$ is given by the Fermi Golden Rule

$$W_{k \rightarrow k'} = \frac{2\pi}{\hbar} g_p^2 \sum_{n=1}^N |a_{k,n}|^2 |a_{k',n}|^2 (\bar{n}_p(T) + 1) \frac{d\rho}{dE}, \quad (8)$$

where $d\rho/dE$ is the density of the phonon states at the frequency of the transition. The above equation is valid for phonon emission ($E_k > E_{k'}$), while for phonon absorption ($E_k < E_{k'}$) the factor $\bar{n}_p(T) + 1$ is replaced by $\bar{n}_p(T)$. It is also convenient to define a function

$$v(E) \equiv \frac{2\pi g_p^2}{\hbar} \frac{d\rho}{dE}, \quad (9)$$

which enters Eq. (8) and carries all the information about the molecular vibrations. In our model we consider this function, which is a product of the exciton–phonon interaction, to be constant.

The kinetics of the exciton states population $P_k(t)$ is described by a Pauli Master Equation

$$\dot{P}_k = -\gamma_k P_k + \sum_{k'=1}^N (W_{k' \rightarrow k} P_{k'} - W_{k \rightarrow k'} P_k), \quad (10)$$

where the dot denotes the time derivative and $\gamma_k \sim \bar{\mu}_k^2$ is the spontaneous emission rate of the k th excitonic state.

Time-dependent fluorescence spectra can be obtained from the solution of Eq. (10), with energy transfer rates calculated via Eq. (8), as

$$I(E, t) = \frac{1}{N} \left\langle \sum_{k=1}^N \gamma_k P_k(t) \cdot L(E - E_k) \right\rangle. \quad (11)$$

3. Simulation method

The molecular arrangement was simulated by a two-dimensional molecular cluster with a square-matrix structure [11]. The size of the clusters used varied from 10×10 to 30×30 . We assumed that the transition dipole of each molecule lies on the same plane and the distance between the adjacent molecules is 10 \AA . The transition moment dipole length in the extended dipole approximation was assumed constant and equal to 3 \AA . All realizations were assumed to take place in room temperature ($T = 200 \text{ cm}^{-1}$). The diagonal disorder

D_n followed a Gaussian distribution, with a typical standard deviation of 500 cm^{-1} . The monomer position was fixed to 22800 cm^{-1} for donors and varied from 17000 to 21000 cm^{-1} for acceptors (traps). The spontaneous emission rate for the donor states was $\gamma = 0.0025 \text{ ps}^{-1}$, and for the acceptor $\gamma_t = 0.01 \text{ ps}^{-1}$. For each aggregate and due to the random disorder we performed 1000–10 000 independent realizations. On each realization of the disorder the Hamiltonian in Eq. (1) was constructed and numerically diagonalized. Using the eigenstates and the eigenenergies we calculated the spectra of the given system and finally averaged our calculated quantities over all different realizations performed.

It was shown previously [11,12] that the above-mentioned molecular arrangement with a tilt angle of the dipole moment $30\text{--}40^\circ$ relative to the x -axis and a magnitude of the dipole moment from 8 to 10 D gives a good agreement of the calculated absorption spectrum with experiments for J-aggregates consisting of pseudoisocyanine dyes, thiacyanocyanine dyes with different meso-substituent, thiacyanine dyes, and oxacyanine dyes. Thus, this molecular arrangement can be used as a good starting point for the calculation of time-dependent luminescence spectra.

The aggregate excitation was due to short impulse pumping, through a delta function $\delta(t)$, in the blue wing of the absorption spectra (24500 cm^{-1}). Eq. (10) was then solved numerically for each realization of the disorder and the time-dependent fluorescence spectra have been calculated via Eq. (11).

We also considered the case of the CW pumping in the same wavenumber. In this case, instead of the time-dependent differential Eq. (10) we have solved the linear algebraic equation, assuming $\dot{P}_k = 0$ in Eq. (10).

For the calculations we also need to know the energy dependence of the phonon density for dye aggregates. Experiments with neutron scattering in aromatic molecular crystals [13,14] showed that the phonon density curves have complicated structure, related to the existence of several vibrational modes and cover the wide energy range from tens to several thousand per centimeter. We assume the function $v(E)$ defined in

Eq. (9) to be constant and equal to W_0 in the energy interval $0\text{--}6000\text{ cm}^{-1}$, while outside this interval it is equal to 0. The value of the constant is considered as a parameter in the calculation, proportional to the strength of the exciton–phonon interaction. Our results are not sensitive to the exact value of the upper energy limit as long as it exceeds the gap between the lower edge of the donor exciton zone and acceptor states. The above-mentioned assumption seems to be reasonable for large dye organic molecules [13,14].

4. Results

4.1. Static spectra

In studies of the CW fluorescence spectra we have seen that different values of the exciton–phonon interaction parameter W_0 drastically influence the fluorescence spectra. For small W_0 values the peak of the fluorescence spectrum is situated at the blue wing of the absorption spectrum, while the fluorescence from the acceptor is absent. With increasing W_0 the peak is shifted to the red side and the fluorescence from the acceptor molecule grows. This shift illustrates the competition of two processes: (i) depopulating each excitonic state of the donor aggregate, and (ii) the luminescence and the intra- and interband energy transfer. For largest W_0 values there is only one fluorescence peak, due to the acceptor.

Comparison of the calculated and experimental luminescence spectra provides the possibility to evaluate the strength of the exciton–phonon interaction. In a recent experiment [15] it was shown that for the mixed aggregates of two dyes 3,3′ Dusulfopropyl-5,5′dicloro-thiacyanine sodium salt (Donor) and 3,3′ dusulfopropyl-5,5′dicloro-9-ethyl-thiacarbocyanine potassium salt (Acceptor I) with the small molar mixing ration of acceptor $\chi_A=0.0133$ there is almost no fluorescence from the donor aggregate and the fluorescence of the acceptor has a $\sim 400\text{ cm}^{-1}$ red shift from the peak of the absorption spectra of acceptor aggregate. This picture corresponds to a value of $W_0=10^9\text{ cm}^{-1}$ in the calculations, and this is the value we used for the calculations in this paper.

Nearly the same results were obtained for another acceptor molecule 3,3′ dusulfopropyl-5,5′dicloro-9-methyl-thiacarbocyanine ethyl ammonium salt (Acceptor II) with $\chi_A=0.00789$. Thus, in the presence of a small impurity of the acceptor molecules in the mixed aggregate, the rate of energy transfer is much higher than the deactivation of excitonic states by spontaneous emission.

It is interesting, thus, to understand what processes give the greatest contribution to the energy transfer mechanism.

The calculated absorption spectra of the system are presented in Fig. 1, for varying disorder strength and varying energy level of the trap. In Fig. 1a, we can see that in the absence of disorder the spectrum consists of a large number of isolated peaks. Increasing disorder leads to a significant broadening of the donor band. The acceptor peak is red-shifted relative to the acceptor monomer energy. This red-shift increases as the acceptor monomer energy increases, as is shown in Fig. 1b, while at the same time the intensity of this peak decreases. When the trap energy is $21\,000\text{ cm}^{-1}$ the red-shift is more than 500 cm^{-1} and the peak has developed into a wider band.

4.2. Time-resolved spectra

In all the absorption spectra of Fig. 1, we can see that there is a significant gap between the donor exciton zone and the acceptor. Thus, this is the case of the persistent type aggregate [12] where the overlap of the wave functions for donor and acceptor states is very small. Despite this gap, the efficiency of the energy transfer to acceptor is high. The energy funneling from the top of the donor exciton zone (where pumping occurs) to the acceptor consists of two parts: inside the donor zone (intraband) and between the two zones (interband). In Fig. 2 we present a graph of the calculated rates for energy transfer from different initial to final excitonic states for a system (a) without disorder and (b) one realization of strong disorder. The energy transfer rate is defined as

$$WE_{k \rightarrow k'} = W_{k \rightarrow k'}(E_k - E_{k'}). \quad (12)$$

In the case of disorder, we can see that the energy transfer to the trap is almost uniformly

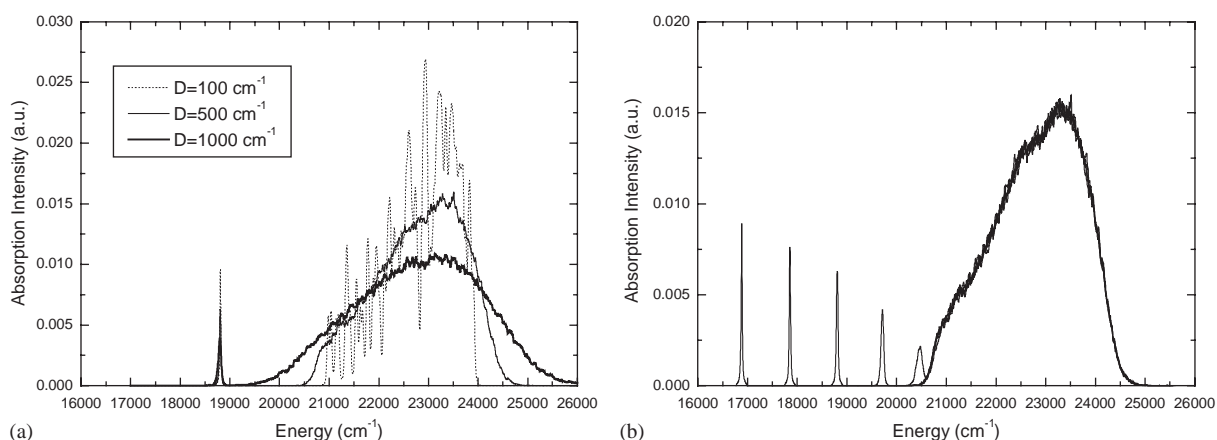


Fig. 1. Calculated absorption spectra for (a) varying disorder strength D and trap energy $E_t = 19,000 \text{ cm}^{-1}$, and (b) varying trap energy E_t and disorder $D = 500 \text{ cm}^{-1}$. In (b) the trap energy is (left to right): 17,000, 18,000, 19,000, 20,000, and 21,000 cm^{-1} .

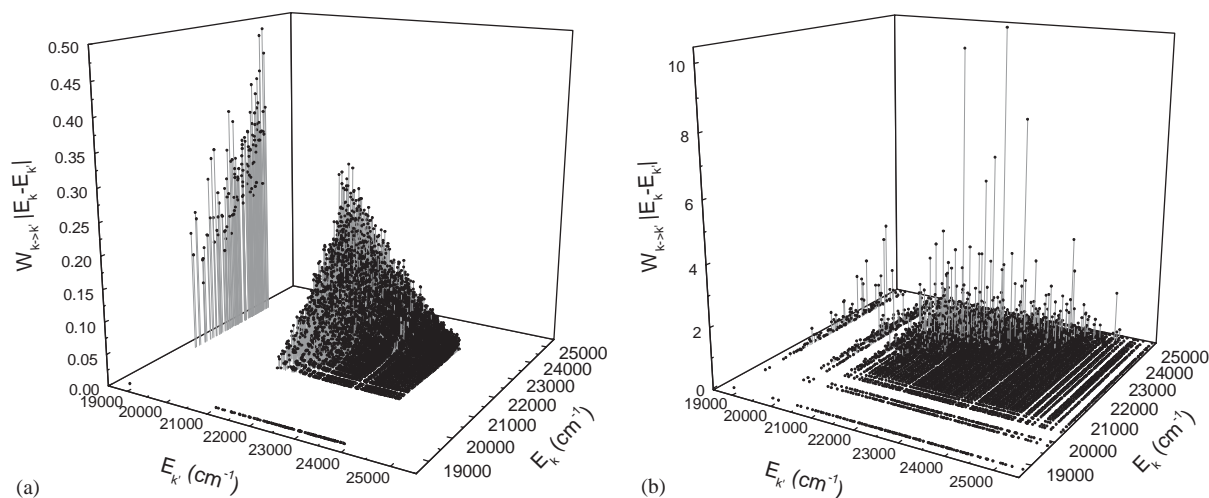


Fig. 2. Energy transfer rates from an eigenstate with energy E_k towards an eigenstate of energy $E_{k'}$, for a system (a) without disorder $D=0$, and (b) with static disorder $D=1000 \text{ cm}^{-1}$.

distributed from the whole donor exciton zone and the intraband energy transfer is much faster than the interband transfer because the density of states in the donor zone is an order of magnitude higher than the corresponding value in the acceptor zone. This relationship is present only in the case of disorder, where excitonic states are localized (the average delocalization length for excitons in the donor zone is ~ 8 – 10 molecules, as is found from the participation ratio). In the case of zero

disorder the delocalization length equals the molecular cluster size and the relationship between intra- and interband energy transfer is different. In Fig. 2a we can also see that the transfer rates of interband transfer are significantly higher than the rates for intraband transfer and the magnitude of the rates is nearly two orders lower than in the case of important disorder. The sharp reduction of the energy transfer rates has two reasons. First, for short aggregates the energy difference for adjacent

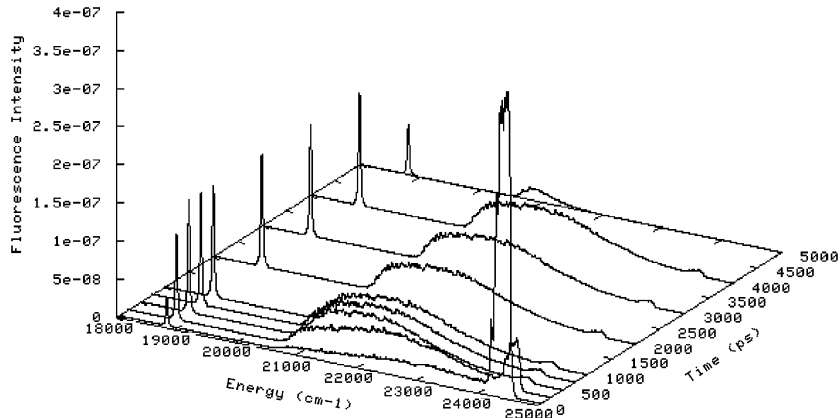


Fig. 3. Time evolution of the fluorescence spectrum for $D = 500 \text{ cm}^{-1}$ and $E_t = 19,000 \text{ cm}^{-1}$.

states is larger. In a one-dimensional aggregate with nearest-neighbor interactions only and for large N this difference is proportional to N^{-2} . For two-dimensional aggregates this difference is proportional to $N^{-2} \log(N)$. The second reason is that the overlap of the wave functions, which is responsible for interstate energy transfer, is also higher for short aggregates. Consider the example of two aggregates with $N=2$ and having one common molecule. In this case the coefficients are $a_{k,1} = a_{k,2} = 1/\sqrt{2}$ and according to formula (10) the overlap is proportional to $\frac{1}{4}$. For longer aggregates with $N=10$ the overlap would be proportional to $\frac{1}{100}$.

For the study of the spectral evolution with time we consider the case of a short pulse excitation, corresponding to a recent experiment where the pulse width of the excitation light was $\sim 1 \text{ ps}$ [15].

In Fig. 3 we can see the time evolution of the fluorescence spectrum. After the initial excitation of the upper exciton states at $24\,500 \text{ cm}^{-1}$ there is a rapid energy transfer towards the red wing of the donor band and towards the trap band. This is also a manifestation of the intra- and interband transfer, as observed also in Fig. 2. Notice also that although the acceptor is excited only through interband energy transfer this excitation is almost immediate. Thus, the acceptor band is populated directly from the upper states, even before the lower donor states have been adequately populated. The fluorescence spectrum reaches a dy-

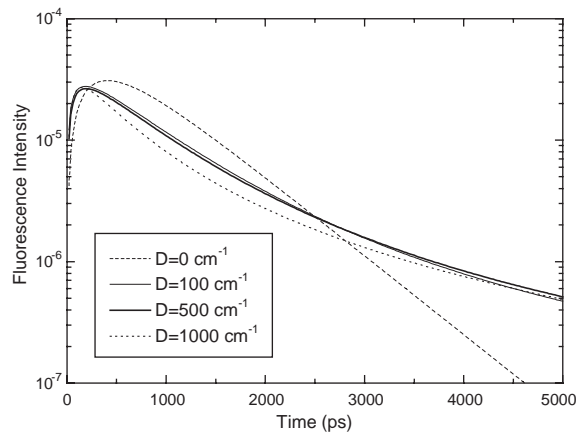


Fig. 4. Time-resolved fluorescence decays from an acceptor at $E_t = 19,000 \text{ cm}^{-1}$ for varying disorder strengths.

namic equilibrium state where it retains its shape, until the spontaneous emission process causes the complete depopulation of the states.

The calculated fluorescence decay of the acceptor is presented in Fig. 4 for different values of the disorder D . In the absence of disorder the fluorescence relaxation is almost exponential, and decays rapidly. The presence of disorder has two main effects: the maximum intensity is slightly lower and occurs at earlier times and the decay is no longer exponential, but follows a slower rate.

Acknowledgments

A.L. acknowledges support from the Russian Fund of Basic Research (Grants 03-02-16817, 04-02-17040 and 03-02-16734) and a collaboration NATO grant (Athens).

References

- [1] F.C. Spano, J. Knoester, In: W.S. Warren (Ed.), *Advances in Magnetic and Optical Resonance*, Academic Press, New York, 1994.
- [2] J. Knoester, F.C. Spano, In: T. Kobayashi, (Ed.), *J-Aggregates*, World Scientific, Singapore, 1996.
- [3] L.K. Gallos, A.V. Pimenov, I.G. Scheblykin, M. Van der Auweraer, G. Hungerford, O.P. Varnavsky, A.G. Vitukhnovsky, P. Argyrakis, *J. Phys. Chem. B* 104 (2000) 3918.
- [4] M. Bednarz, V.A. Malyshev, J. Knoester, *Phys. Rev. Lett.* 91 (2003) 217401.
- [5] M. Bednarz, V.A. Malyshev, J. Knoester, *J. Chem. Phys.* 120 (2004) 3827.
- [6] M. Shrieber, Y. Toyozawa, *J. Phys. Soc. Japan* 51 (1982) 1528.
- [7] V. Czikkely, H.D. Försterling, H. Kuhn, *Chem. Phys. Lett.* 6 (1970) 207.
- [8] H. Fidder, J. Knoester, D.A. Wiersma, *J. Chem. Phys.* 95 (1991) 7880.
- [9] J.A. Leegewater, J.R. Durrant, D.R. Klug, *J. Phys. Chem. B* 101 (1992) 408.
- [10] J.P. Lemaistre, *Chem. Phys.* 246 (1999) 283.
- [11] A.G. Vitukhnovsky, A.N. Lobanov, A.V. Pimenov, Y. Yonezawa, N. Kometani, *Int. J. Mod. Phys. B* 15 (2001) 4017.
- [12] A.G. Vitukhnovsky, A.N. Lobanov, A. Pimenov, Y. Yonezawa, N. Kometani, K. Asami, J. Yano, *J. Lumin.* 87-89 (2000) 260.
- [13] E.L. Bokhenkov, I. Natkanets, E.F. Sheka, *JETP Lett.* 33 (1981) 497.
- [14] V. Malyshev, P. Moreno, *Phys. Rev. B* 51 (1995) 14587.
- [15] N. Kometani, H. Nakajima, K. Asami, Y. Yonezawa, O. Kajimoto, *J. Phys. Chem. B* 104 (2000) 9630.